RSC Advances

ROYAL SOCIETY OF CHEMISTRY

www.rsc.org/advances

RSC Advances

ARTICLE

A new strategy for simultaneous determination of 4-aminophenol, uric acid and nitrite based on graphene/hydroxyapatite composite modified glassy carbon electrode

N. Lavanya[a],N. Sudhan[a], P. Kanchana[a], S. Radhakrishnan[b] and C. Sekar[a]*

Received 00th January 20xx,
Accepted 00th January 20xx

DOI: 10.1039/x0xx00000x

www.rsc.org/

A novel electrochemical sensor has been fabricated based on graphene/hydroxyapatite nanocomposite modified glassy carbon electrode (GCE) for the selective and simultaneous detection of 4-aminophenol (4-AP), uric acid (UA) and nitrite ion (NO^{2-}) in phosphate buffer solution (PBS, pH 7.0) for the first time. The modified electrode exhibited an improved electrocatalytic activity towards the oxidations of 4-AP, UA and NO^{2-} in the form of three strong peaks in both cyclic voltammetry (CV) and square wave voltammetry (SWV) techniques. Under optimum conditions, the ternary system comprising 4-AP, UA and NO^{2-} exhibited linear calibration plots over wide range of 0.1-425 µM, 1-1000 µM and 3-950 µM with detection limits of 0.29 µM, 0.03 µM and 0.025 µM for 4-AP, UA and NO^{2-} respectively. The developed sensor displayed high sensitivity and low detection limits coupled with good stability and reproducibility which were attributed to the synergistic effect of graphene and HAP in the nanocomposite. In addition, the fabricated sensor was applied to the determination of UA, 4-AP and NO^{2-} in urine and tap water samples with satisfactory results.

1. Introduction

4-Aminophenol (4-AP) is the primary hydrolytic degradation product of acetaminophen, and has been detected in pharmaceutical preparation of acetaminophen as a synthetic intermediate. 4-AP is also broadly applied in production of dyestuff, developer, chemical inhibitor and petroleum additive. As a result, large amounts of 4-AP may be inevitably released into the environment as a pollutant [1]. Due to the discoveries of its significant nephrotoxicity and teratogenic effect, the maximum content of 4-AP in pharmaceuticals is limited to 50 ppm (0.005 %, w/w) by the European [2] and United States [3] pharmacopeia. The overdose of 4-AP is the foremost cause of acute liver failure and account for most morbidity and mortality in drug-poisoning cases. Hence, precise determination of 4-AP in matrices such as water, pharmaceutical formulations and human fluids is important [4].

Nitrite (NO^{2-}) is ubiquitous with environmental, food and life science and commonly used as food additive, fertilizing agents and corrosion inhibitor. Excessive nitrite in the body can lead to the irreversible oxidation of hemoglobin to methemoglobin; furthermore, nitrite can react with amine to form a carcinogenic nitrosamine, resulting in cancer and hypertension. The World Health Organization has reported that the fatal dose of nitrite ingestion is between 8.7 µM and 28.3 µM [5,6]. Recently, many studies have demonstrated that NO could act as a neurotransmitter or a neuromodulator in central nervous system, and also, NO could enhance or inhibit the release of dopamine [7, 8]. Moreover, NO can be oxidized to NO^{2-} within a few seconds by reacting with the dissolved oxygen in solution and also in the biological environments [9]. Hence, precise determination of NO^{2-} is important requirement for medical and environmental applications.

Uric acid (UA) is known to be an important natural antioxidant in blood and brain tissue scavenging superoxide, peroxynitrite and hydroxyl radical. The typical concentrations of UA is in millimolar range (120– 450 $\mu molL^{-1}$) in blood and about 2 $mmolL^{-1}$ in urine and its abnormality can lead to some diseases like gout, hyperpiesia, and Lesch–Nyhan disease. Higher serum UA levels have been associated with a significantly reduced risk of Parkinson disease, low levels linked to multiple sclerosis [10]. Therefore, it is necessary to develop a simple, fast and sensitive analytical method for simultaneous detection of 4-AP, UA and NO^{2-} for both environmental and biomedical benefits. Recently, electrochemical techniques have been used extensively due to its advantageous features such as high sensitivity, fast response, inexpensive instrument, low energy consumption, simple operation, time saving, good reliability and possibility for in-situ analysis. The

[a]*Department of Bioelectronics and Biosensors, Alagappa University, Karaikudi-630003,Tamilnadu, India.*

[b]*Nanomaterials and System Lab, Department of Mechanical System Engineering, Jeju National University, Jeju 690-756, Republic of Korea*

E-mail: Sekar2025@gmail.com, Tel:9194425663637;

Electronic Supplementary Information (ESI) available: [details of any supplementary information available should be included here]. See DOI: 10.1039/x0xx00000x

4-AP, UA and NO^{2-} contain electrochemically active groups which can be oxidized independently at different potentials. So, various electrochemical sensors were reported for their analysis. For instance, graphene/polyaniline [11], graphene/chitosan [12], single walled nanotube/nafion [13], hemim based molecular imprinted polymer [14] modified elctrodes were reported for the detection of 4-AP. As for the detection of UA and NO^{2-}, their simultaneous determination was achieved using $La(OH)_3$ nanorods [15], poly(2-mercaptobenzothiazole) [16], lanthanum multiwalled carbon nanotube nanocomposites [17], Au-nanoclusters incorporated 3-amino-5-mercapto-1,2,4-triazole film [18], and thiazole-based copolymer [19] modified electrodes. However, to the best of our knowledge, there has been no report for the simultaneous determination of all the three molecules viz. 4-AP, UA and NO^{2-}. In this work, we have fabricated a graphene/hydroxyapatite composite modified glassy carbon electrode for the selective and simultaneous determination of 4-AP, UA and NO^{2-} for the first time.

Graphene have attracted considerable attention due to its extraordinary mechanical, thermal, electrical properties, fast electron transportation and good biocompatibility which makes it suitable for potential applications in the field of electrochemical sensors, solar cells and energy storage capacitors [20-22]. Hydroxyapatite (HAP, $Ca_{10}(PO_4)_6(OH)_2$) is a form of calcium phosphate that bears close chemical likeness with the mineral part of bone and teeth. It promotes tissue attachment and bone growth by spontaneously forming a biologically active bone-like apatite layer on its surface. Thus, HAP is classified as a biocompatible and bioactive material and crystalline HAP has been found in many biological applications such as dental or skeletal implants, bone repair scaffolds, and biosensors [23]. The HAP and graphene nanohybrids are important kinds of nanocomposite materials which successfully integrate the unique properties of two classes of materials and exhibit some new functions caused by the cooperative effects between the HAP and the graphene such as high electron mobility and excellent catalytic activity. Recently, graphene/HAP nanocomposites have been synthesized and their potential applications in bioactive and biomedical fields have been demonstrated [25].

Here, we report the synthesis of graphene/HAP composite by a simple chemical precipitation method and demonstrated its applicability as sensing material for the simultaneous detection of three important molecules 4-AP, UA and NO^{2-}. The graphene/HAP modified GCE not only exhibits high electrocatalytic activities toward the oxidations of 4-AP, UA and NO^{2-} with enhanced oxidation peak currents, but also resolve the sluggish and over-lapped oxidation waves at GO/GCE into three well-defined anodic peaks. Thus, the simultaneous determinations of 4-AP, UA and NO^{2-} in human urine and tap water samples have been investigated as real sample applications.

2. Experimental

2.1 Materials

The reagents used were of analytical grade without further purification. Graphite, sulfuric acid, potassium permanganate, 4-aminophenol, uric acid, sodium nitrite and hydrogen peroxide (H_2O_2, 30% w/v solution) were purchased from Sigma Aldrich. Calcium nitrate tetrahydrate ($Ca(NO_3)_2.4H_2O$), diammonium hydrogen phosphate ($(NH_4)_2HPO_4$), trisodium citrate and cetyltrimethyl ammonium bromide were obtained from Merck. 0.1 M phosphate buffer solution (PBS) was prepared by dissolving appropriate amounts of sodium hydrogen phosphate and sodium dihydrogen phosphate. The pH of the buffer was adjusted to appropriate value by adding hydrochloric acid. All electrochemical experiments were carried out in 0.1 M PBS at pH 7.0. Freshly prepared 4-AP, UA and NO^{2-} solution were used for each experiment.

2.2 Instrumentation

Powder X-ray diffraction (XRD) analyses were carried out on a Bruker D8-ADVANCE diffractometer with Cu Kα radiation of wavelength (λ) of 0.15418 nm. The morphology of the samples was checked by scanning electron microscope (SEM) (FEG QUANTA 250). The functional groups of graphene/HAP nanocomposite were identified by recording Fourier Transform Infrared (FTIR) spectra (Thermo Nicolect 380) and Raman spectra at room temperature (Princeton Instruments Acton SP2500 (0.5 m imaging triple grating monochramator/spectrograph)).

Electrochemical measurements were carried out using a CHI 608d electrochemical workstation (CH Instruments, Austin, USA). A three-electrode system was employed with a 3 mm glassy carbon (GC) as the working electrode, a Pt wire as the auxiliary electrode and Ag/AgCl (saturated KCl) as the reference electrode in an electrochemical cell filled with 10 mL of PBS at room temperature. Electrochemical impedance spectroscopy (EIS) experiment was performed in 0.1 M KCl containing 1 mM $[Fe(CN)_6]^{3-/4}$. The EIS experiments were carried out by applying an ac potential of amplitude 5 mV over the dc potential of 200 V in the frequency range of 100 kHz to 1 Hz. Cyclic voltammograms (CVs) were recorded between a potential window from -0.2 V to 1.2 V at the scan rate of 50 mV/s in 0.1 M PBS (pH 7.0) containing 4-AP, UA and NO^{2-}. Square wave voltammetry (SWV) measurements were performed in PBS (pH 7.0) in the potential region from -0.2 to 1.2 V with frequency of 10 Hz, amplitude of 50 mV and step potential of 5 mV.

2.3 Synthesis of graphene oxide (GO)

The graphene oxide (GO) was prepared according to modified Hummer's method [26]. Briefly, 1g graphite was added to 50 mL of concentrated sulfuric acid cooled by an ice water bath. Then 4g potassium permanganate was slowly added and the mixture was stirred at 30°C for 1 h. Next, 150 mL water was added, and the mixture was stirred for 30 min while the temperature was raised to 90°C. Finally, 200 mL water was added, followed by the slow addition of 3 mL of H_2O_2 (30%), turning the color of the solution from dark brown to greenish yellow. The solid graphite oxide was separated by centrifugation, washed repeatedly with deionized water and finally dried under vacuum.

2.4 Synthesis of the graphene/HAP composite

Graphene/HAP nanocomposite was synthesized by a simple chemical precipitation method [27]. In brief, dried GO

(2 mg) was dispersed in deionized water (1 mL). Then (40 wt%) 94 mg of $Ca(NO_3).4H_2O$ was added into 90 mL of GO colloid solution with ultrasonic treatment for 60 min to form a colloidal suspension. Subsequently 40 mg of cetyltrimethylammonium bromide (CTAB) was added into solution and sonicated for 60 min to form solution A. Approximately 103.2 mg of trisodium citrate and 31.56 mg of $(NH_4)_2HPO_4$ were added into 15 mL of ultrapure water to form solution B which was poured into solution A. The combined solution was sonicated for 30 min and then kept in hot air oven at 180°C for 12 hrs. The composite was washed several times with ethanol and water in order to remove CTAB and trisodium citrate ions and the product was dried at 60 °C for 24 h.

2.5 Fabrication of the modified electrodes

Glassy carbon electrode (GCE) was polished carefully with 1.0, 0.3 and 0.5 µM alumina on polishing cloth and was rinsed with deionized water which was followed by successive ultrasonic treatment to remove the physically adsorbed substance. Graphene/HAP composites (5.0 mg) were dispersed in 1 mL deionized water by using ultrasonicator. Then, 10 µL of the prepared suspension was dropped onto the GCE surface by drop casting method and dried in room temperature to obtain the graphene/HAP modified GCE (Scheme 1). In addition, GO and HAP modified GC electrodes were prepared by the above mentioned process for comparison.

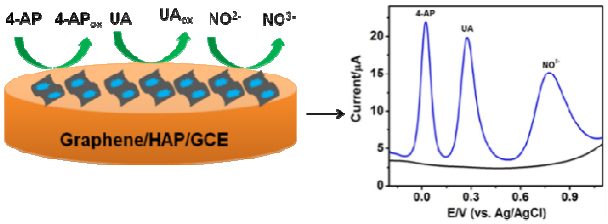

Scheme1. Schematic representation of the graphene/HAP modified GC electrode for simultaneous detection of 4-AP, UA and NO^{2-}

3. Results and Discussion

3.1 Structural analysis

Powder X-ray diffraction pattern of GO shows a diffraction peak (Figure 1A.a) at around 10.87° (2θ), which corresponds to the (002) reflection of stacked GO sheets. HAP shows diffraction peaks corresponding to hexagonal structure with space group P63/m (ICDD card no. 09–0432) as shown in Figure 1A.b [23]. No obvious diffraction peaks attributed to graphite in the XRD pattern of the graphene/HAP nanocomposite are observed. This result indicates that the HAP adhered on graphene sheets can prevent stacking into multilayers, favouring the maintenance of high surface area. Figure 1B shows the SEM image of (a) GO, (b) HAP and (c) graphene/HAP nanocomposite. The characteristic plate like morphology was clearly seen for pure HAP. However, when GO is introduced, HAP plates anchored on a wrinkled GNS as shown in Figure 1B.b.

Figure 1C shows the Raman spectra of (a) GO and (b) graphene/HAP nanocomposite. The peak observed at about 1590 cm^{-1} (G band) corresponding to E_{2g} mode of graphite, was related to the vibration of the sp^2-bonded carbon atoms in a 2 dimensional hexagonal lattice, while the peak at about 1357 cm^{-1} (D band) was related to the breathing of k point phonons of A_{1g} symmetry [28]. The intensity ratio of the D to G band (I_D/I_G) was calculated as 1.05 and 1.1 for GO and graphene/HAP nanocomposite respectively. Compared with GO, the intensity ratio of ID/IG for graphene/HAP is increased, which could be ascribed to the exfoliation of GO and the presence of HAP between the GO.

The FTIR spectra of (a) GO, (b) graphene/HAP and (c) HAP are shown in Fig. 1D. In case of composite sample, an absorption band located at ~3420 cm^{-1} is due to O–H vibrations of absorbed water and the bands located at 562 cm^{-1}, 603 cm^{-1} are assigned to the PO_4^{3-}. The oxygen-containing functional groups of GO were revealed by the presence of bands at 1089, 1227, 1633, and 1730 cm^{-1}. These bands can be assigned to the C–O stretching vibration, C–OH stretching vibration, C=C stretching vibration, and C=O stretching vibration of COOH group, respectively [17].The absorption bands at 1033, 565 and 602 cm^{-1} are attributed to characteristic absorption of PO_4^{3-} in HAP.

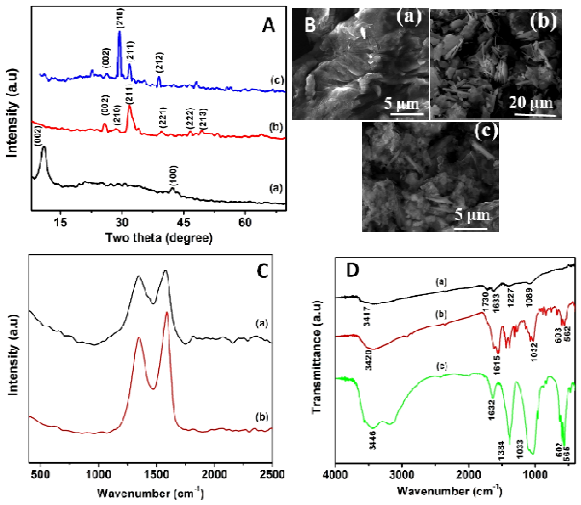

Figure 1 (A) XRD patterns of (a) GO, (b) HAP and (c) graphene/HAP and (B) SEM image of (a) GO, (b) HAP and (b) graphene/HAP; (C) Raman spectra of (a) GO and (b) graphene/HAP; (D) FTIR spectra of (a) GO, (b) graphene/HAP and (c) HAP.

3.2 Electrochemical activity of graphene/HAP nanocomposite modified GC electrode

The charge transport process of the graphene/HAP modified GC electrode was studied by monitoring charge transfer resistance (Rct) at the electrode/electrolyte interface. The R_{ct} values were obtained by Randels equivalent circuit, $R_s(Q_{CPE}(R_{ct}W))$, where R_s is the solution resistance, R_{ct} is the charge transfer resistance, W is the Warburg impedance and Q_{CPE} is the constant phase element (CPE). Figure S1A shows the electrochemical impedance spectroscopy (EIS) responses of the bare and modified GC

electrodes. The R_{ct} values for the bare GC (curve a), GO (curve b), HAP (curve c) and graphene/HAP (curve d) modified electrodes were estimated to be 705, 4125, 1506 and 310 Ω cm^{-2} respectively. It can be noticed that the R_{ct} value of graphene/HAP/GCE is lower than that of bare GC, GO and HAP modified electrodes which demonstrate that the graphene/HAP modified electrode can form good electron pathways between the electrode and electrolyte and that it can be a good platform for sensing applications. These results are in good agreement with the peak current (i_{pa}) values obtained from CV measurements (Figure S1B).

Figure S1B shows the cyclic voltammograms (CVs) of different modified electrodes recorded in the presence of 1 mM $Fe(CN)_6]^{3-/4-}$ in 0.1 M KCl at the scan rate 50 of mV/s. Well-resolved anodic and cathodic peaks are observed at the bare GCE (curve a), GO (curve b) HAP (curve c) and graphene/HAP (curve d) modified GC electrodes. Compared to those obtained at the bare GCE (17 µA), GO/GCE (2 µA) and HAP/GCE (16 µA), a significantly higher peak current was obtained at the graphene/HAP (35 µA) modified GC electrode. The peak separation potential (ΔE) of the redox peaks for graphene/HAP/GCE and HAP/GCE are obtained as 91 and 203 mV, respectively which indicate the fast electron transfer process capability of the graphene/HAP/GCE. These observations aptly suggest that the graphene/HAP based electrode is more facile than the bare, GO and HAP modified GC electrodes.

3.3 Electrochemical behavior of 4-AP, UA and NO^{2-}

The individual electrochemical behavior of 4-AP, UA and NO^{2-} in PBS (pH 7.0) at bare GCE (curve a), GO/GCE (curve b), HAP/GCE (curve c) and graphene/HAP/GCE (curve d) were first investigated by cyclic voltammetry (CV) studies. In the case of 0.1 mM 4-AP (Figure 2A), a small defined redox wave appeared at the bare electrode (curve a). On the other hand, modification GC electrode with graphene/HAP significantly enhances the oxidation peak current of 4-AP (7.5 µA) which is 2-fold higher relative to that of bare GCE (3.7 µA) and HAP (2.6 µA) modified GCE. The modified graphene/HAP/GCE not only improves the redox peak currents but also makes the redox reaction of 4-AP more reversible which shows that the modified GCE plays an important role in accelerating the electron transfer toward the detection of 4-AP. For UA (0.5 mM) oxidation (Figure 2B), a sluggish and much smaller anodic peak response was observed at the bare GCE. On the other hand, the graphene/HAP/GCE exhibits a sharp and strong oxidation peak at 0.30 V with greatly increased peak current response (16.2 µA), which is 18-fold higher than that of the bare GCE (0.9 µA). In the case of 0.5 mM NO^{2-} (Figure 2C), the bare GCE shows a small and broad oxidation peak at 0.9 V; whare as, a strong anodic peak appears at a more negative potential of 0.8 V at the graphene/HAP modified GC electrode. Moreover, about 1.2-fold increase in anodic peak current (14.7 µA) is observed in comparison with that at bare GCE (12 µA). These results indicate that, among the three investigated electrodes, the graphene/HAP/GCE possesses the best electrocatalytic properties towards the oxidation of 4-AP, UA and NO^{2-}, which demonstrate the synergistic effect of the reduced GO and HAP in the hybridcomposite.

The effect of scan rate on the electrochemical responses of 4-AP, UA and NO^{2-} at the graphene/HAP modified GCE was studied by CV. As demonstrated in Figure S2, the anodic peak currents of the analytes increase linearly with the scan rate (υ) over the range of 50–500 mV s^{-1}. The linear equations for 4-AP, UA and NO^{2-}have been deduced as (i_{pa}= 0.8221$\upsilon^{1/2}$-1.088, R^2 = 0.9935), (i_{pa}=0.17696$\upsilon^{1/2}$+3.8244, R^2 = 0.9955), (i_{pa}= 1.2426$\upsilon^{1/2}$+ 2.586, R^2 = 0.9974) respectively. The results indicate that the electrode reactions of all the three investigated analytes at the graphene/HAP/GCE are of diffusion-controlled processes.

3.4 Voltammetric separation of 4-AP, UA and NO^{2-}

In order to understand the electrochemical behavior of 4-AP, UA and NO^{2-}in the mixture solution, CVs were recorded at GO/GCE (curve a), HAP/GCE (curve b) and graphene/HAP/GCE (curve c) respectively and the results are shown in Fig. 2D. At the GO/GCE, the oxidation peaks of 4-AP and UA completely overlap with each other leading to a broad oxidation peak at 0.6 V which revealed that it is impossible to deduce any information from this peak. On the other hand, when the graphene/HAP modified GC electrode was used, the overlapped voltammetric peak was resolved into three well-defined CV peaks at 0.01 V, 0.38 V and 0.75 V, corresponding to 4-AP, UA and NO^{2-}respectively. The peak potential separations for 4-AP–UA and UA-NO^{2-} were 0.37 mV and 0.37 mV at the graphene/HAP/GCE, which were large enough for the selective and simultaneous determinations of 4-AP, UA and NO^{2-} in their mixture. These results reaffirm that the graphene/HAP/GCE not only enhances the oxidation of 4-AP, UA and NO^{2-}, but also dramatically enlarge the peak separation among 4-AP, UA and NO^{2-}. The enlarged separation of the anodic peak potential, coupled with the increased sensitivity, indicates that the simultaneous determination of 4-AP, UA and NO^{2-}in the co-existence system is feasible. Hence we have used of graphene/HAP modified GC electrode for further investigations.

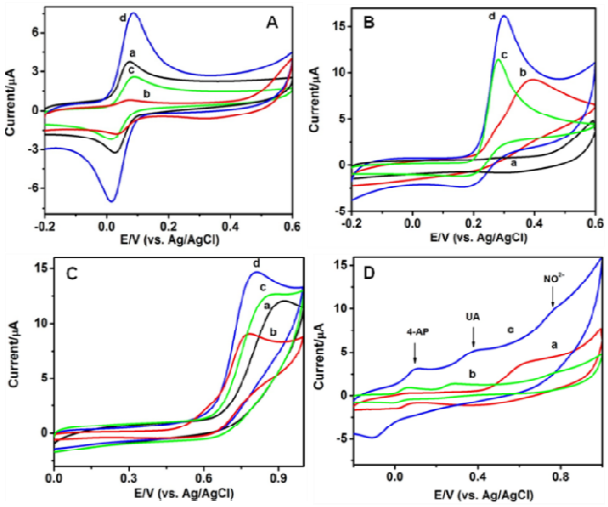

Figure 2 (A) Cyclic voltammograms of (A) 0.1 mM 4-AP (B) 0.5 mM UA and (C) 0.5 mM NO^{2-} in 0.1 M PBS (pH 7.0) at (a) bare, (b) GO, (c) HAP and (d) graphene/HAP composite modified GCE at a scan rate of 50 mV/s.; (D) CVs obtained for the mixture of 25 µM 4-AP, 50 µM UA and 50 µM NO^{2-} in 0.1 M PBS (pH 7.0) at (a) GO (b) HAP and (c) graphene/HAP composite modified GCE at a scan rate of 50 mV/s.

3.5 Selective determinations of 4-AP, UA and NO^{2-} by SWV

SWV technique was employed for the selective determinations of 4-AP, UA and NO^{2-} in their mixture due to its higher sensitivity and better resolution than the CV method. For individual determination of 4-AP, UA and NO^{2-} at the graphene/HAP/GCE, SWV was carried out in the potential range of −0.2 to 1.0 V in PBS (pH 7.0). As shown in Figure 3**,** a series of SWV curves were obtained by changing the concentration of one molecule while keeping the concentrations of the other two as constant. The results shown in Figure 3A–C indicate that the peak currents for the oxidations of 4-AP, UA and NO^{2-} increase proportionally with their concentrations. For 4-AP, the linear relationship between the peak current and its concentration is obtained in the range of 0.1–50 µM and 50–425 µM (Figure 3D, and the linear regression equation is calibrated as (0.1 – 50 µM) I_{pa} = $0.112c_{4\text{-}AP}$ + 4.27 (R^2 = 0.997); (50 – 420 µM) I_{pa} = $0.067c_{4\text{-}AP}$ +6.88 (R^2 = 0.996). In Figure 3E, the oxidation peak current of UA increases with the increase of its concentration in the range of 1–50 µM and 50–1000 µM. The corresponding linear function is (1–50 µM) I_{pa}= $0.0467c_{UA}$+ 0.928 (R^2 = 0.996); (5–0.1 mM) I_{pa}= $0.0208c_{UA}$+2.90 (R^2 = 0.995). Similarly (Figure 3F), the peak current of NO^{2-} increases linearly with the increase of its concentration with the linear function (3-50 µM) I_{pa}= $0.0527c_{NO^{2-}}$+ 1.43 (R^2 = 0.997); (50 – 950 µM) I_{pa}= $0.0122c_{NO^{2-}}$+ 3.72 (R^2 = 0.995). The lowest detection limits (LODs) are estimated as 0.29 µM, 0.03 µM and 0.025 µM for 4-AP, UA and NO^{2-} respectively based on the lower concentration range. The linear range and detection limit for 4-AP, UA and NO^{2-}at graphene/HAP/GCE were compared with the recently reported values for similar chemically modified electrodes (Table 1). These results demonstrate that individual determination of 4-AP, UA and NO^{2-} can be achieved with high sensitivity and selectivity at the graphene/HAP/GC electrode.

Table 1 Comparison of different chemically modified electrodes for th determination of 4- AP, UA, NO^{2-} with graphene/HAP/GCE

Electrode	4-AP	UA	NO^{2-}	4-AP	UA	NO^{2-}	Ref
	Linear range (µM)			Detection limit (µM)			
[a]GR/Polyaniline	0.2–100	-	-	0.065	-	-	11
[b]GR Chitosan	0.2–550	-	-	0.050	-	-	12
[c]SWNT-nafion	0.005-2	-	-	0.008	-	-	13
[d]MIP	10–90	-	-	3	-	-	14
[e]$La(OH)_3$	-	0.05-790	0.55-720		0.001	0.18	15
[f]PMBT	-	1-165	60-1000	-	0.10	0.30	16
[g]La/MWCNT	-	0.04-810	0.4-710	-	0.015	0.13	17
[h]Au-p-A/GCE	-	1.6-110	15.9-277	-	0.08	0.89	18
[i]PATA	-	1.9-1200	2-1240	-	0.25	0.5	19
[j]GR/HAP	1-140	1-840	1-840	0.90	0.35	0.52	This work

[a] Graphene-polyaniline modified GCE
[b]Graphene- Chitosan modified GCE
[c] Singled walled carbon nanotube modified GCE
[d]Hemim based molecular imprinted polymer modified GCE
[e] $La(OH)_3$ nanorods modifed GCE
[f]Poly(2mercaptobenzothiazole) modified GCE
[g]Lanthaum/multiwalled carbon nanotube modified GCE
[h]Au nanoclusters/3-amino-5-mercapto-1,2,4-triazole modified GCE
[i]Thiazole-based copolymer modified GCE
[j]Graphene/hydroxyapatite modified GCE

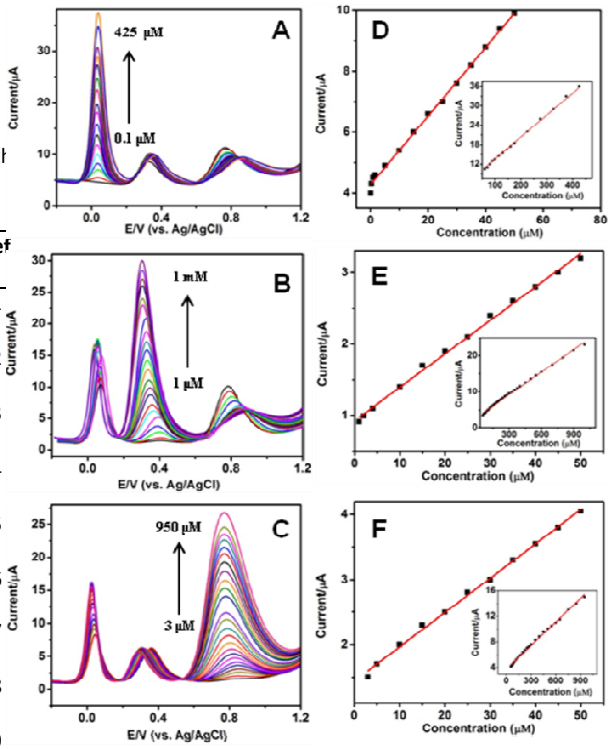

Figure 3 (A) SWVs obtained for various concentrations 4-AP (0.1 to 425 $\times10^{-6}$ M) at graphene/HAP modified GCE in the presence of 200 µM each UA and NO^{2-} in 0.1 M PBS (pH 7.0), (B) SWVs obtained for various concentrations of UA (1 to 1000 $\times10^{-6}$ M) at graphene/HAP modified GCE in the presence of 200 µM each 4-AP and NO^{2-} in 0.1 M PBS (pH 7.0), (C) SWVs obtained for various concentrations NO^{2-} (3 to 950$\times10^{-6}$ M) at graphene/HAP modified GCE in the presence of 200 µM each 4-AP and UA in 0.1 M PBS (pH 7.0) and Figure 3 (D E F) represents the corresponding calibration curves.

3.6 Simultaneous determinations of 4-AP, UA and NO^{2-}

To investigate the possibility of using the graphene/HAP modified GC electrode for simultaneous determinations of 4-AP, UA and NO^{2-}, the SWV peak current responses of these species for various concentrations in the mixture have been measured. It can be seen from Figure 4A that the peak currents for oxidations of 4-AP, UA and NO^{2-} increase proportionally with their concentrations. The linear ranges for the determinations of 4-AP, UA and $NO^{2-}$are found to be 1- 140 µM, 1 - 840 µM and 1 - 840 µM with detection limits of 0.90 µM, 0.35 µM and 0.52 µM respectively. The linear regression equations for 4-AP, UA and NO^{2-}were obtained as I_{pa} = $0.146c_{4\text{-}AP}$ + 3.261 (R^2 = 0.995); I_{pa} = $0.0319c_{UA}$ + 3.17 (R^2 = 0.995) and I_{pa}= $0.112c_{NO^{2-}}$ + 3.50 (R^2 = 0.995) respectively. These results demonstrated that the graphene/HAP composite modified GC electrode provide a good electrocatalytic activity towards simultaneous detection of the three important chemical species 4-AP, UA and NO^{2-}. Moreover, graphene/HAP composite preparation and electrode modification procedure adopted in the present study are very simple and highly reproducible.

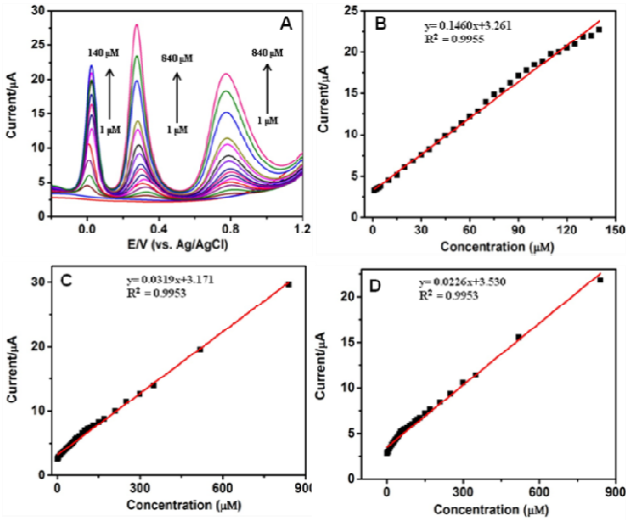

Figure 4 (A) SWVs obtained for various concentrations of 4-AP (1 -140 µM), UA (1 - 840 µM) and NO^{2-}(1 - 840 µM.) at graphene/HAP/GCE in 0.1 M PBS (pH 7.0) and (B), (C) & (D) are plots of the oxidation peak currents as a function of various concentrations of 4-AP, UA and NO^{2-}.

3.7 Interference, reproducibility and stability studies

The anti-interferent ability of the graphene/HAP/GCE was investigated by detecting its response to the mixture of 4-AP, UA and NO^{2-} in the presence of several common co-exiting substances. The results indicate that the presence of 10 times ascorbic acid and 100 times of K^+, Na^+, Ca^{2+}, Mg^{2+} and glucose have no influence on peak currents of 4-AP, UA and NO^{2-}. The reproducibility of the proposed biosensor was determined with four different electrodes. The relative standard deviations (RSD) of the current responses were 1.6%, 2.5% and 1.8% for 4-AP, UA and NO^{2-} respectively. The storage stability of the modified electrode was investigated over a period of 30 days by storing it in 0.1 $molL^{-1}$ PBS (pH 7.0) at room temperature. There were no obvious changes in the current response during the first week, and the response decreased to 97.0% of the initial value after 10 days, and it further got reduced to 92.5% after 20 days and this response remained nearly stable thereafter.

3.8 Determination of 4-AP, UA and NO^{2-} in real samples

Human urine and tap water samples were selected for real sample analysis using the standard addition method. The developed sensor was applied to test 4-AP and NO^{2-} in tap water and UA in urine samples respectively. Solutions were prepared by adding 4-AP and NO^{2-} in tap water and analyzes were done without any prior treatment. The results are shown in Table 2. The human urine samples were diluted 50 times with 0.1 M PBS without any other treatment. The dilution process helps to reduce the matrix effect of real samples. SWV response was measured after different concentrations of UA standard solution was added into 10 mL 0.1 M PB solution (pH 7.0) and the results are presented in Table 3. Figure 5 shows typical SWV responses obtained at graphene/HAP/GCE from tap water and urine samples containing 4-AP, NO^{2-} and UA respectively. The peak current responses were found to regularly increase upon standard addition of 4-AP, NO^{2-} and UA. It can be clearly seen that a good recovery has occurred in all the three investigated samples. The results suggest that the proposed method could be effectively used for the determination of 4-AP, UA and NO^{2-}in real samples.

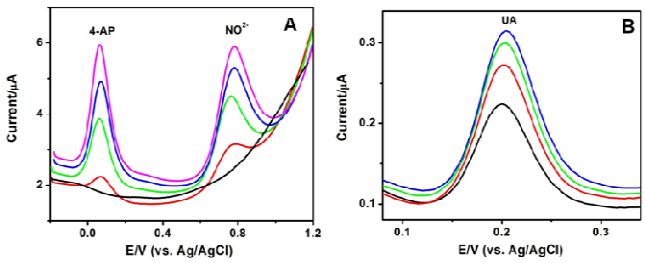

Figure 5. SWVs obtained at graphene/HAP/GCE from (A) tap water and (B) human urine samples containing 4-AP, NO^{2-} and UA respectively.

Table 2 Determination of 4-AP and NO^{2-} in tap water using graphene/HAP/GCE

Sample	Added (μM)	Found (μM)	RSD (%) (n=3)	Recovery (%)
4-aminophenol (4-AP)				
1	2	2.1	3.61	98.2
2	4	3.8	2.70	97.6
3	10	9.7	0.59	101.2
Nitrite (NO^{2-})				
1	1	1.8	2.46	102.3
2	5	5.7	2.04	97.5
3	10	9.8	1.57	98.5

Table 3 Determination of UA in human urine sample using graphene/HAP/GCE

Sample	Added (μM)	Found (μM)	RSD(%) (n=3)	Recovery (%)
1	5	6.2	1.61	104.5
2	10	12.4	0.96	99.8
3	15	17.5	0.88	102.3

3. Conclusions

An electrochemical sensor for the simultaneous determination of 4-AP, UA and NO^{2-} have been realized for the first time using graphene/HAP hybrid composite modified GCE. The fabricated electrode exhibited high electrocatalytic activities towards the oxidation of 4-AP, UA and NO^{2-} with well separated strong peaks at 0.02, 0.27 and 0.77 V respectively. Compared with the electrodes made of either GO and HAP independently, their hybrid graphene/HAP composite modified GCE facilitate the simultaneous determinations of 4-AP, UA and NO^{2-} with high sensitivity and selectivity. The oxidation peak currents of the three compounds depend linearly on the concentrations over the range of 0.1−420 μM for 4-AP, 1−1000 μM for UA and 3−900 μM for NO^{2-} with the lowest detection limits of 0.29 μM, 0.03 μM and 0.025 μM respectively. With such excellent features as wide linear dynamic range, high sensitivity and selectivity, the developed sensor provides a new strategy for determination of 4-AP, UA and NO^{2-} in biomedical and environmental samples with satisfactory results.

Acknowledgements

Authors NL & CS acknowledge the Council of Scientific and Industrial Research (CSIR No.03(1203)/12/EMR-II) and University Grants Commission (UGC. F. No. 40-2/2011) for the financial assistance. P.K acknowledges the University Grants Commission (UGC) for providing the Post Doctoral Fellowship (No. F.15-1/2011-12/PDFWM-2011-12-OB-TAM-2867 (SA-II)). N. Sudhan acknowledges the DST-PURSE for financial support.

References

[1]T. Nemeth, P. Jankovics, J.N. Palotas and H.H. Szalai, *J. Pharm. Biomed. Anal.*2008, **47**, 746 -752.
[2]The European Pharmacopeial Convention, The sixth edition European Pharmacopoeia, 2007, 49.
[3]The United States Pharmacopeial Convention, The United States Pharmacopoeia 27-NF (The National Formulary) 2004, 2494.
[4]A. Safavi, N.Maleki, O.Moradlou, *Electroanalysis,*2008,**20**, 2158.
[5]Y.G. Huang, J.D. Ji and Q.N. Hou, *Mutat. Res*. 1996, **358**, 7.
[6]S. Radhakrishnana, K. Krishnamoorthy, C. Sekar, J. Wilson and S.J. Kim, *Appl. Catal., B*. 2014, **148–149**, 22.
[7]G. Lonart, J. Wang and K.M. Johnson, *Eur. J. Pharmacol.*1992, **220**,271.
[8] G. Lonart, K.L. Cassels and K.M. Johnson, *J. Neurosci. Res.*1993, **35**, 192.
[9] R. Guevara-Guzman, P.C. Emson and K.M. Kendrick, *J. Neurochem.*1994**, 62**, 807.
[10] P. Kalimuthu and S.A. John, Bioelectrochemistry, 2009, **77,** 13.
[11] Y. Fan, J.H. Liu, C.P. Yang, M. Yu and P. Liu, *Sen.Actuators B-Chem.* 2011, **157**, 669.
[12] H. Yin, Q. Ma, Y. Zhou, S. Ai and L. Zhu, *Electrochim. Acta*, 2010, **55**, 7102.
[13] W. Huang, W. Hu and J. Song, *Talanta*, 2003, **61**, 411.
[14] J.R.M. Neto, W.J.R. Santos, P.R. Lima, S.M.C.N. Tanaka, A.A. Tanaka and L.T. Kubot, *Sen.Actuators B-Chem.* 2011,**152**, 220.
[15] Y. Zhang, R. Yuan, Y. Chai, X. Zhong, and H. Zhong, *Colloids &Surf.,B,*2012, **100***,* 185.
[16] L. Zhang and D. Yang, *Electrochim. Acta,* 2014,**119**,106.
[17] W. Zhang, R. Yuan, Y.Q. Chai, Y. Zhang, S.H. Chen, *Sens. Actuators B–Chem.*2012, **166 – 167**, 601.
[18] C. Wang, R. Yuan, Y. Chai, Y. Zhang, F. Hu and M. Zhang, *Biosen. Bioelectron*. 2011, **30,** 315.
[19] L. Zhang, D. Yang and L. Wang, *Electrochim. Acta,* 2013**,111**, 9.
[20] T. Kuila, S. Bose, P. Khanra, A.K. Mishra, N.H. Kim and J.H. Lee, *Biosen.Bioelectron.*2011**, 26**, 4637.
[21] X. Wang, L.J. Zhi and K. Mullen, *Nano Lett.2008*, **8**, 323.
[22] O.Barbieri, M.Hahn, A.Herzog and R. Kotz, *Carbon,* 2005**, 43,** 1303 - 1310.
[23] P.Kanchana, N.Lavanya and C.Sekar, *Mater.Sci. Eng. C*, 2014**,35**, 85.
[24] H. Zanin, E. Saito, F-R. Marciano, H.J. Ceragioli, A. Eustaquio, C. Granato, M. Porcionattod and A-O. Lobo, *J. Mater. Chem. B.*2013, **1**, 4947.
[25] Y. Liu, J. Huang and H. Li, *J. Mater. Chem. B.* 2013, **1**, 1826.
[26] S. Gilje, S. Han, M. Wang, K. L. Wang and R. B. Kaner, *Nano Lett*. 2007, **7**, 3394.
[27] Z. Fan, J. Wang, Z. Wang, H. Ran, Y. Li, L. Niu, P. Gong, B. Liu and S. Yang, Carbon, 2014, **66**, 407.
[28] K.S. Subrahmanyam, S.R.C. Vivekchand, A. Govindaraj, and C.N.R. Rao, *J. Mater. Chem. B,* 2008, **18**, 1517.

Graphical Abstract